Colloid Polym Sci (2003) 282: 103–109
DOI 10.1007/s00396-003-0917-y

ORIGINAL CONTRIBUTION

F. Becerra
J.F.A. Soltero
J.E. Puig
P.C. Schulz
J. Esquena
C. Solans

Free-radical polymerization of styrene in worm-like micelles

Received: 23 September 2002
Accepted: 28 March 2003
Published online: 7 October 2003

F. Becerra · J.F.A. Soltero (✉) · J.E. Puig
Departamento de Ingeniería Química,
CUCEI, Universidad de Guadalajara,
Boul. M. García Barragán 1451, 4430
Guadalajara, Jal., Mexico
E-mail: jfasm@hotmail.com
Fax: + 52 33-36-19-40-28

P.C. Schulz
Departamento de Química,
Universidad Nacional del Sur,
8000 Bahía Blanca, Argentina

J. Esquena · C. Solans
Departament deTecnologia de Tensoactius,
Institut d'Investigacions Químiques i
Ambientals de Barcelona,
Consejo Superior de Investigaciones
Científicas, C/Jordi Girona 18–26,
08033, Barcelona, Spain

Abstract The solubilization of styrene in wormlike micelles of the cationic surfactant, cetyltrimethylammonium tosilate (CTAT), and its polymerization is examined here by UV spectroscopy, oscillatory rheometry, small angle X-ray scattering, polarizing light microscopy, and transmission electron microscopy. At low CTAT concentrations, the polymerization of styrene yields small and rigid rods in coexistence with wormlike micelles that form from the excess surfactant after the polymerization process. At high CTAT concentrations, polymeric rods (of large aspect ratio), spheroid polymer particles, and wormlike micelles coexist. The polymerization rate is second order, indicating that polymerization reactions end mainly by bimolecular termination.

Introduction

Surfactants can form a wealth of fluid microstructures in water, as well as in polar and non-polar solvents [1, 2]. However, because surfactant self-aggregation is controlled by thermodynamics [3], changes in temperature, salinity, pH, etc., modify these microstructures. Hence, there is an interest in "freezing" these microstructures through polymerization to produce polymers with unique shapes and for special applications, such as microencapsulation, controlled drug delivery, membranes with controlled nano-porous size, etc. [4]. Microstructure freezing can be achieved by the polymerization of monomers previously solubilized in the microstructure or by polymerization of the microstructure made with polymerizable surfactants [4, 5, 6, 7, 8]. Even though the latter approach has been favored, successful *microstructure locking in* has been achieved by the polymerization of monomers dissolved in surfactant-based fluid microstructures. McKelvey et al. fixed bilayers by polymerizing divinylbenzene solubilized in vesicles [9]. Gan et al. produced membranes with nano-pores of narrow size distribution by the polymerization of bicontinuous microemulsions containing monomers, water and polymerizable surfactants [10, 11]. These authors showed that the pores of the membranes were larger and less uniform when a conventional surfactant was employed.

Wormlike micellar solutions are of scientific and technological interest because they are viscoelastic, even at very dilute surfactant concentrations [12, 13]. The reason for this behavior is that they can form entanglements similar to polymer solutions. However, since they can break and reform continuously, wormlike micellar solutions exhibit more complex linear and nonlinear viscoelastic behaviors than those of polymer solutions [14, 15, 16].

Polymerization of spherical micelles has been attempted but the resulting polymer particles are larger than the original micelles or form elongated structures [8, 17]. Polymerization of rod-like micelles, on the other hand, has been scarcely attempted. Kline was able to partially preserve the rod-like structure by polymerizing a wormlike micellar solution of the polymerizable surfactant, cetyltrimethylammonium 4-vinylbenzoate [18]. He determined from SANS that the resulting polymer rods had similar diameters to those of the original rods, but they were much shorter.

Here we report the polymerization of styrene solubilized in wormlike micelles of the cationic surfactant, cetyltrimethylammonium tosilate (CTAT). Our results, supported by rheology, SAXS, polarizing light microscopy, and TEM indicate that the microstructure is partially preserved. To our knowledge, this is the first time that a successful freezing of the wormlike micellar microstructure has been achieved by this method.

Experimental section

Cetyltrimethylammonium tosilate (CTAT), 98% pure from SIGMA, was recrystallized from chloroform (analytical grade from Aldrich). Styrene or ST (99% pure from either Scientific Polymer Products or Merck) and divinylbenzene or DVB (from Aldrich) were either passed through a DRH-7 silica gel column (SPP) to remove the inhibitor or distilled under vacuum. The photoinitiator, benzoin isobutylether, was 99% pure from Aldrich. 2,2'-Azobisisobutyronitrile (AIBN), 98% pure from Dupont, was recrystallized from methanol. Water was drawn from a Milli-Q reagent water system or a Millipore purification system.

Samples were made by two different procedures. In one, CTAT and water were weighed (5 and 25 wt.% CTAT), mixed by hand several times every day for a few days, and then allowed to reach equilibrium at 30 °C in a water bath. Styrene or styrene/DVB (98/2 by weight) was then added to the vial, shaken several times, and allowed to rest in a water bath at 30 °C for at least 72 h. The other procedure consisted in weighing all components (CTAT, water, and monomers) in glass tubes with a narrow neck in its middle part. These tubes were sealed with a torch and kept at constant temperature in a thermostatic bath. Everyday the samples were withdrawn from the bath and centrifuged four times at 2000 rpm for 5 min, turning around the tube to force its content through the narrow neck. This process was repeated for several days until complete homogenization was observed. Then, the tubes were kept at constant temperature for 3 days without further centrifugation.

The polymerization was carried out in a rectangular box provided with temperature controlled (30 ± 0.1 °C) and c.a. 90°-four UV lamps. The lamps (General Electric F15T/BLB) have a maximum emission peak at 354 nm with 15 W total potency. Samples (20 mL each) contained in sealed Pyrex tubes were bubbled through with nitrogen for 5 min before the irradiation process started. Then the tubes were put into the box and retired at different times to follow the reaction kinetics. The polymer was isolated by precipitation with methanol and washed repeatedly with double distillated water to eliminate all the remaining CTAT.

Dynamic oscillatory measurements were performed at 30 °C in a Rheometrics RDS-II spectrometer with a cone-and-plate geometry. The cone angle and plate diameter were 0.1 rad and 50 mm, respectively. To minimize water loses during the tests, a humidification chamber surrounded the cone-and-plate fixture.

To determine the location of the styrene molecules in the micelles, UV spectra of styrene dissolved in solvents of different dielectric constants (n-tetradecane, water/methanol mixtures and water with 1 wt.% urea to facilitate its dissolution) were taken in a UV-visible Lambda IV spectrometer (Perkin-Elmer). Quartz cuvettes of 1 mm in path length were used. The UV spectra of styrene solubilized in 0.02 and 0.5 wt.% CTAT micellar solutions were taken using CTAT solutions of the same concentrations as blanks to eliminate the absorption peaks of the tosilate group since it absorbs at similar wavelengths than styrene.

Average molar masses and molar mass distributions (MMD) of resulting polymers were obtained in a Perkin Elmer gel permeation chromatograph equipped with a refractive index (Perkin Elmer) and a multi-angle light scattering (Wyatt Technology) detectors. HPLC-grade tetrahydrofurane (Merck) was used as the mobile phase.

X-Rays for small angle scattering (SAXS) were produced by a K-760 Siemens generator at a power of 2 kW. Samples were placed in Mylar film cells because some of them were very viscous and could not be placed in glass capillaries, and then thermostated with an AP PAAR temperature controller (± 0.5°C) Peltier device. The collimation was carried out with a Kratky camera (HECUS Mbraum-Graz) and the scattering was detected with a PSD-50 position sensitive detector (HECUS Mbraum-Graz). The intensity, reported in arbitrary units because the peak height depends on the Mylar cell thickness, was represented as a function of the scattering vector, $q\ [= (4\pi/\lambda)\sin(\theta/2)]$ in a range of 0.04 to 0.6 Å^{-1}. The water and Mylar scattering vector were subtracted by measuring the background, and the smearing was corrected in all measurements.

The microstructures of the polymerized samples were obtained in a Hitachi 600 AB transmission electron microscope, operating at a acceleration voltage of 75 kV. Samples were diluted 6 times in an acidic solution of uranyl acetate (2 wt.% at pH 4.2) and a small drop (≈ 5 μL) of the solution was placed on a Formvar carbon coated copper grid and dried at room temperature. Similar results were produced by first placing a small amount of sample on the grid, drying at room temperature, and then adding a drop of the acidic solution of the uranyl acetate.

Results and discussion

The 5 and 25 wt.% CTAT solutions were chosen because they are representative of the semi-dilute and concentrated regimes where entangled wormlike micelles form [19]. Both solutions are transparent and highly viscous. Upon addition of styrene up to a weight ratio of styrene to CTAT (w_{St}/w_{CTAT}) of 0.1, solutions remain transparent and viscous, although less viscous than the parent solutions. Above this ratio, and up to 0.14, samples become bluish and even less viscous. For w_{St}/w_{CTAT} higher than 0.14, two layers appear. The upper layer is bluish and fluid whereas the bottom one is milky and much more viscous. The interface is not sharp but

rather diffuse and remains like that for months, because phase separation is very slow. The volume of the bottom layer increases with increasing styrene concentration.

To determine the structure of the bottom layer, the dispersions were centrifuged at the equilibrium temperature and the bottom layer was sampled and examined by polarizing light microscopy. When the polarizers are crossed, Maltese crosses are seen, whereas vesicles and onion like structures of about 20 μm in diameter were detected without polarizers. These observations confirm the lamellar structure of this phase.

The location of the styrene molecules in the micelles was investigated by examining the UV spectra of 0.02 and 0.5 wt.% CTAT solutions as a function of styrene content. The method uses several styrene spectral features that change with the surrounding environment: (i) the intensity of the 210 nm band, which appears in polar solvents but disappears in non polar solvents, (ii) the details of the fine structure bands between 270 and 300 nm, which are well-defined in non-polar solvents and become less defined as the polarity of the solvents increases, (iii) the form and shape of the band located between 240 and 250 nm, and (iv) the ratio of the absorbance bands at 210 and 250 nm [20, 21, 22]. Figure 1 displays the spectra of styrene in tetradecane (spectrum a) and in water (spectrum b), where the different spectral features are clearly revealed. A plot of A_{210}/A_{250} for styrene as a function of the dielectric constant of the solvent is shown in the inset of Fig. 1. Clearly, this ratio increases as the dielectric constant of the solvent augments.

Figure 2 displays the spectra of styrene in 0.02 and 0.5 wt.% CTAT solutions with increasing styrene content. The spectra of the 0.02% CTAT solutions (Fig. 2a) indicate that some styrene molecules are at the

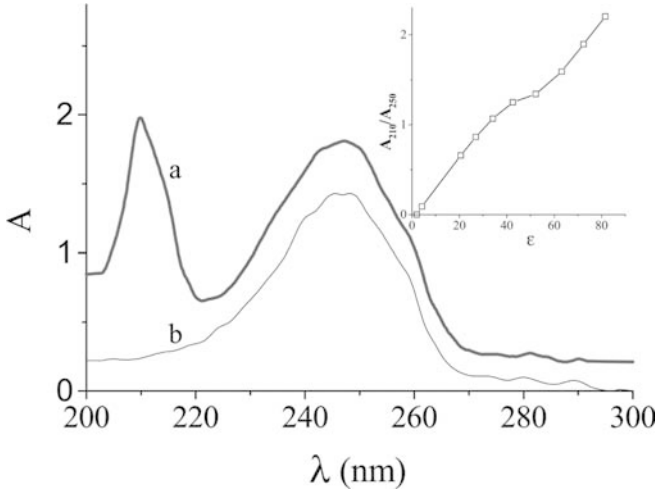

Fig. 1 UV spectra of styrene in water (with 1 wt.% urea) (*a*) and in n-tetradecane (*b*) *Inset*: A_{210}/A_{250} of styrene in solution as a function of the dielectric constant of the solvent

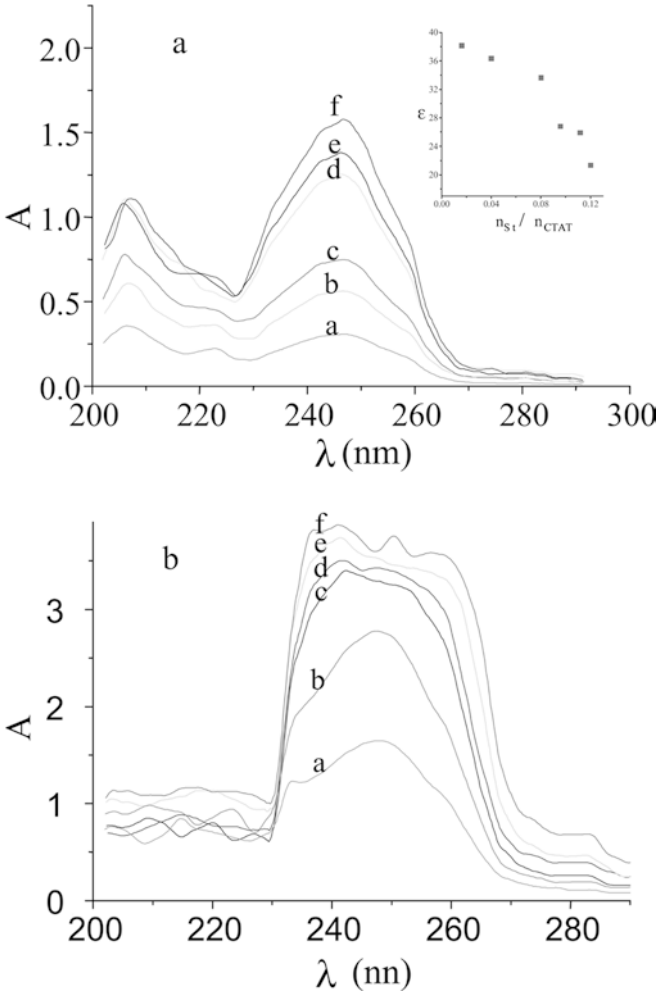

Fig. 2a, b UV spectra of styrene dissolved in **a** 0.02 and **b** 0.5 wt.% CTAT solutions as a function of styrene content at 25 °C. n_{St}/n_{CTAT}: *a* 0.027, *b* 0.047, *c* 0.075, *d* 0.11, *e* 0.13, *f* 0.22. *Inset* in **a**: mean value of the local dielectric constant around the styrene molecules in the 0.02 wt.% CTAT system, as a function of the number of styrene molecules per CTAT molecule in the system

micelle-water interface, and the remainder in the hydrocarbon micelle core, i.e., the resulting spectra are a superposition of both states. This is the so-called *two-state solubilization model* [20, 21, 22]. By using the inset of Fig. 1, the mean value of the local dielectric constant ($\epsilon_{average}$) around the styrene molecules was computed for each styrene/CTAT ratio. The $\epsilon_{average}$ values are represented in inset in Fig. 2a as a function of the number of styrene molecules per CTAT molecule in the system, n_{St}/n_{CTAT}. It is evident that as the n_{St}/n_{CTAT} ratio augments, $\epsilon_{average}$ goes from typical values at the micelle Stern layer ($\epsilon_{average} = 38$–33, [20, 22, 23]) to lower values ($\epsilon_{average} \approx 20$) indicating that some styrene molecules are in the hydrocarbon micelle core.

The absences of the band at 215 nm—characteristic of styrene at or close to the water-surfactant interface,

and of the fine structure at $\lambda > 270$ nm—typical of styrene in a polar environment, and the similarities with the spectrum in tetradecane (Fig. 1) in the spectra of the 0.5 wt.% CTAT solutions (Fig. 2b) indicate that the styrene molecules are located inside the core of the micelles. The difference between the two systems (0.02 and 0.5 wt.% CTAT) may be caused by the different solubilization capacities of the spherical and cylindrical micelles. Larger micelles have larger solubilization capacity than small ones [24]. In the 0.5 wt.% CTAT system the proportion of styrene molecules at the surface was very small and undetectable.

Figure 3 shows SAXS spectra, measured at 30 °C, of 25 wt.% CTAT solutions without and with styrene ($w_{St}/w_{CTAT} = 0.1$) before and after polymerization. The spectrum of the styrene-free sample (spectrum a in Fig. 3) reveals a single broad peak with a maximum at q of approximately 0.1 $Å^{-1}$, which would correspond to structures with a repetitive distance ($2\pi/q$) of about 60 Å. The Porod region ($I \propto q^{-4}$) and the region where $I \propto q^{-1}$, which would confirm the wormlike micellar structure, are not available to the SAXS instrument used here. Therefore, the structure of the aggregates cannot be confirmed but information about the repetitive distance can be deduced from the position of the correlation peak. The SAXS spectrum of the styrene-free sample, taken at 50 °C (not shown), has no significant differences with respect to that taken at 30 °C and therefore, both the repetitive distance and the structure do not change in the studied range of temperatures. SAXS measurements were also carried out at different surfactant concentrations (not shown); in this case, the position of the peak shifted to higher q-values with increasing surfactant concentration, i.e., increasing volume fraction (Φ), as $I \propto \Phi^{0.56}$, which is similar to theoretical predictions [25, 26]. In addition, the intensity of the peak was significantly lower at 5 wt.%, and the level of the noise was higher, because the scattering intensity is proportional to the volume fraction of the aggregates.

Upon addition of styrene below the solubilization limit, the correlation peak moved to lower q-values probably due to the slight growth of the structures (spectrum b in Fig. 3). Upon increasing styrene content, below the solubilization limit, the SAXS spectra (not shown) are very similar to that shown in Fig. 3 for CTAT solutions with styrene, i.e., the peak shifts to about the same q value, which corresponds to an approximate repetitive distance of 65 Å for the aggregates.

Upon polymerization, the spectrum is very similar to that of the solution with styrene (spectrum c in Fig. 3), suggesting that the original structure is preserved with a slight increase in the repetitive distance. Samples with higher polystyrene contents did not reveal any significant additional features. It is noteworthy that both systems (5 and 25 wt.%) are stable and transparent but exhibit a bluish tinge.

Figure 4 depicts the elastic (G') and the viscous (G'') moduli as a function of frequency, measured at 30 °C and strain deformations within the linear viscoelastic region, for the 5 and 25 wt.% CTAT solutions. Both samples are viscoelastic. In the terminal zone, the viscous modulus of the 5 wt.% solution dominates up to frequencies of ca. 1 s^{-1} whereas the elastic behavior extends up to 4 s^{-1} for the 25 wt.% sample. The frequency where G' and G'' crossover (ω_∞) is equal to the inverse of the main relaxation time of the sample. Here τ_R is equal to 0.8 s and 0.25 s for the 5 and 25% samples, respectively. For frequencies larger than ω_∞, the sample response is predominantly elastic. The elastic modulus increases with frequency and reaches a constant value at high frequencies (G_0) whereas the viscous modulus rises with frequency, goes through a maximum, then diminishes and finally increases with frequency with a slope of

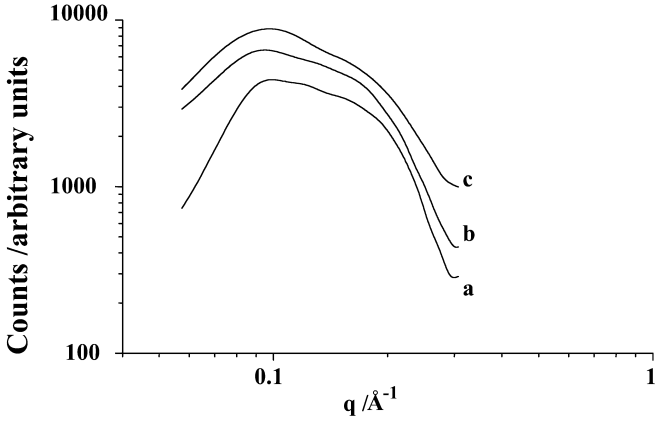

Fig. 3 Small angle x-ray scattering (SAXS) of 25 wt.% CTAT solutions: *a* without styrene, *b* with styrene before polymerization, *c* after polymerization ($w_{St}/w_{CTAT} = 0.1$)

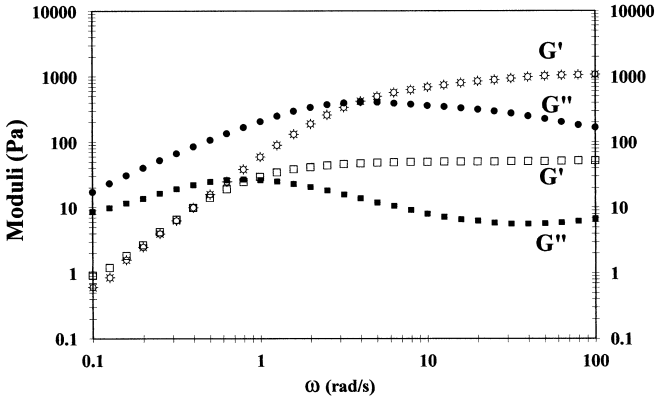

Fig. 4 Frequency sweeps obtained at 30 °C in the linear viscoelastic regime of 5 wt.% (*black squares*, *white squares*) and 25 wt.% (*black dots*, *white suns*) CTAT solutions

1 for both samples. Elsewhere, it is demonstrated that this upturn in G'' is related to occurrence of Rouse modes [14].

Figure 5 presents the elastic and viscous moduli as a function of the frequency at 30 °C for the 5 and 25 wt.% CTAT samples with a St/CTAT = 0.1. The rheological behavior of both samples is predominantly viscous in most of the frequency range examined. In fact, the crossover frequency for the 25% sample shifts to values larger than the available high-frequency range of the rheometer. Both the elastic and the viscous moduli are two decades smaller than those of the solutions free of styrene (cf. Figs. 4 and 5). This could be due for the shortening of the wormlike micelles' length caused by the solubilization of styrene and also to a shifting from *fast*- to *slow* breaking regime inasmuch as the life of the micelles is longer [27]. That these systems are still viscoelastic (i.e., both G' nd G'' are clearly detected) with slopes closer but not quite Maxwellian—because the shifting to the slow breaking regime [14], rules out the disappearance of the wormlike micelles and the formation of swollen spherical micelles.

Upon polymerization, the dynamic moduli change drastically (Fig. 6). Samples are still viscoelastic but G' and G'' have increased to levels near to those of the CTAT solutions without styrene (cf. Figs. 4 and 6). The crossover frequency is clearly observed in both samples and it has shifted to higher values. The main relaxation times of the 5 and the 25 wt.% samples containing polystyrene are 0.6 and 0.1 s, respectively. One should expect that upon polymerization and the formation of rigid rods, the viscoelasticity of the samples should decrease, contrary to rheological results (Fig. 6). However, after polymerization, the overall surface area of the short polystyrene rods should be smaller than that of the parent wormlike micelles. Also, the stability of the resulting polymer suspension suggests that the

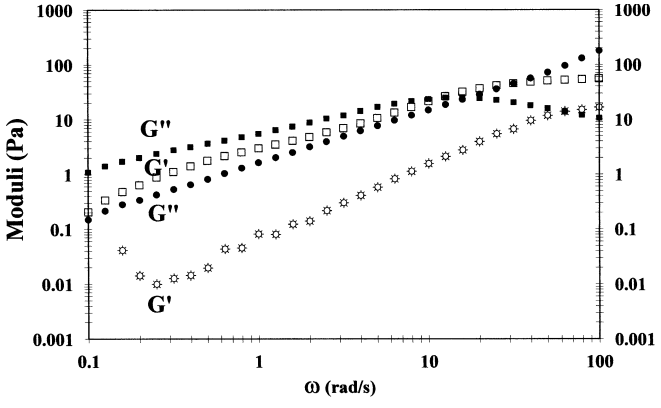

Fig. 5 Frequency sweeps obtained at 30 °C in the linear viscoelastic regime of 5 wt.% (*black squares*, *white squares*) and 25 wt.%(*black dots*, *white suns*) CTAT solutions containing styrene ($w_{St}/w_{CTAT} = 0.1$)

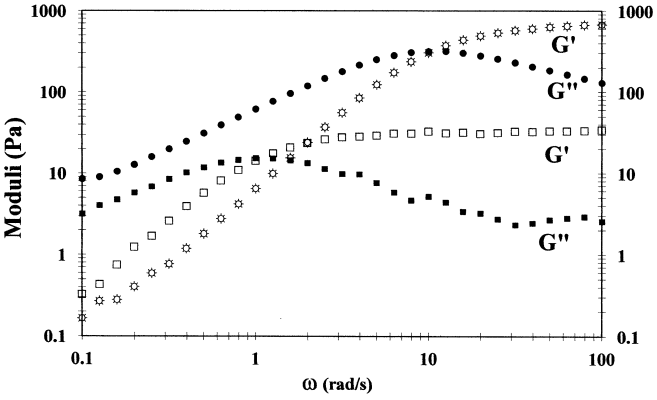

Fig. 6 Frequency sweeps obtained at 30 °C in the linear viscoelastic regime of 5 wt.% (*black squares*, *white squares*) and 25 wt.% (*black dots*, *white suns*) CTAT solutions containing styrene ($w_{St}/w_{CTAT} = 0.1$) after polymerization

polystyrene rods have adsorbed surfactant molecules. Hence, we proposed that the excess surfactant molecules reorganize to form flexible wormlike micelles, which coexist with the rigid polystyrene rods.

The styrene polymerization kinetics for the 5 and 25 wt.% CTAT solutions ($w_{St}/w_{CTAT} = 0.1$) was followed by UV spectroscopy. Figure 7 depicts conversion as a function of time for the 5 (top) and 25% (bottom) samples. Reaction rate is much faster for the 5 wt.% sample and fractional conversions near one are achieved in both samples. The logarithmic plot of the polymerization rate versus the reacted monomer concentration (insets in Fig. 7, top and bottom) is linear with a slope of two, indicating that the order of reaction is 2 for both samples. In radical chain polymerization with low monomer concentration, termination occurs exclusively by primary termination [28]. In the cases examined here, it appears that the termination reactions occur by primary termination. Under such circumstance, the polymerization rate is second order and is given by:

$$R_p = \frac{k_p k_i}{k_{tp}} [M]^2 \tag{1}$$

The average molar masses and the MMD of the polystyrene obtained by polymerization in the wormlike micelles (without the crosslinking agent, DVB) were compared to those obtained by bulk polymerization. The polymer produced after polymerization in the wormlike micelles has a number-average molar mass of 4.2×10^4 Dalton with a narrow polydispersity (M_w/M_n) of 1.41. This value is consistent with termination by coupling. In fact, Odian [28] gives the following formula for the polydispersity as a function of conversions when termination is by coupling:

$$\frac{M_w}{M_n} = \frac{2+p}{2} \tag{2}$$

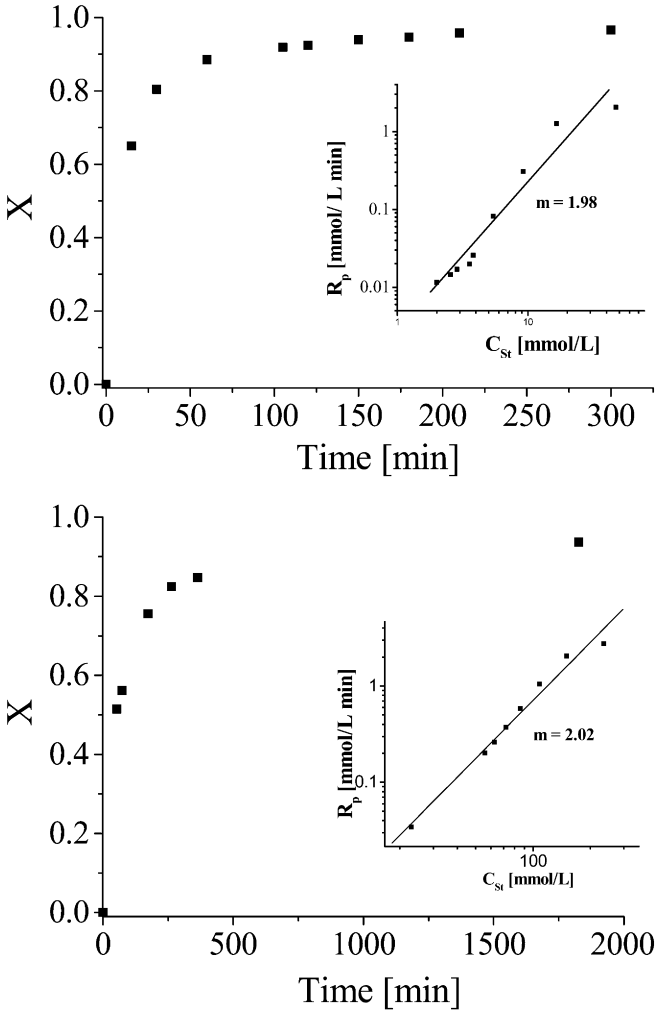

Fig. 7 Conversion as a function of time for the polymerization of styrene in a 5 wt.% (*top*) and 25 wt.% (*bottom*) CTAT samples ($w_{St}/w_{CTAT} = 0.1$). *Insets*: polymerization rate as a function of reacted monomer concentration

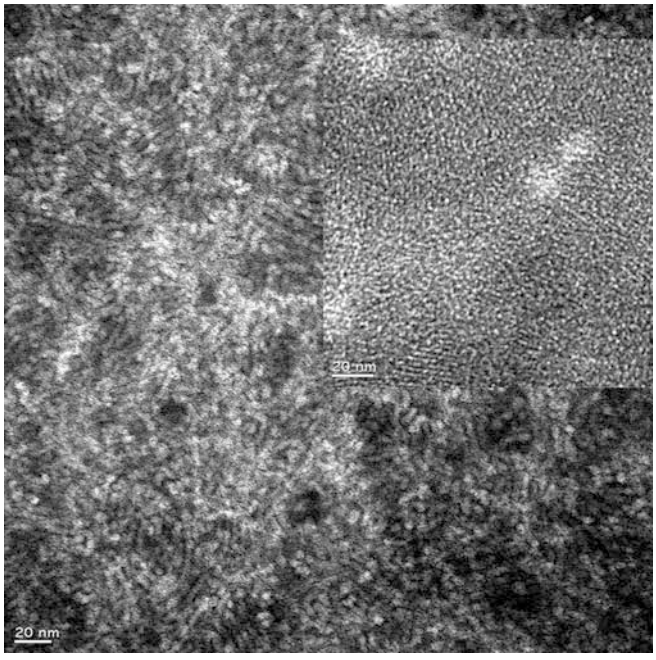

Fig. 8 TEM image of a polymerized sample containing 5 wt.% CTAT and $w_{St}/w_{CTAT} = 0.1$. *Inset*: TEM photograph of the unpolymerized sample

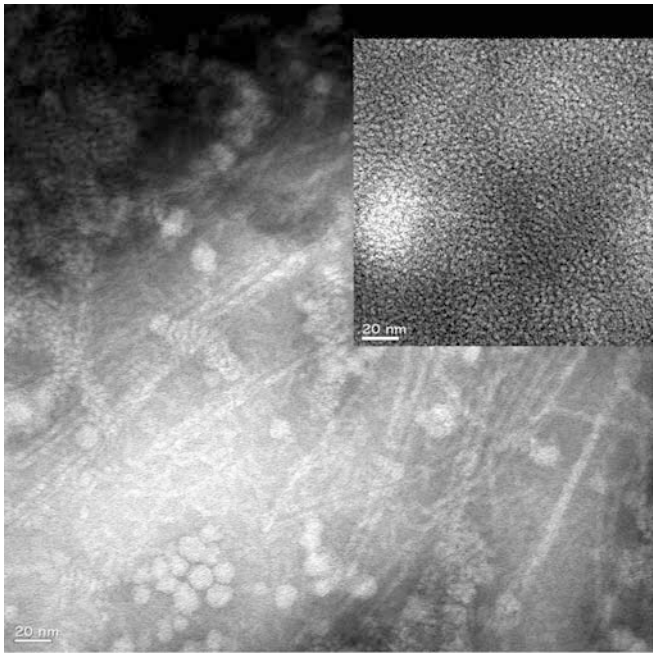

Fig. 9 TEM image of a polymerized sample containing 25 wt.% CTAT and $w_{St}/w_{CTAT} = 0.1$. *Inset*: TEM photograph of the unpolymerized sample

where p is the fractional conversion. In our case, the conversion achieved was ca. 0.98 and so, the expected value is around 1.48, which is similar to the value reported here.

By contrast, the polystyrene obtained by bulk polymerization had a much higher M_w (4×10^5 Dalton) and much broader polydispersity (M_w/M_n) of 18, which is typical of the latter polymerization process [28]. In fact, the values obtained for the polymerization in wormlike micelles are similar to those expected for solution polymerization of styrene in a good solvent [28].

Figures 8 and 9 show TEM photographs of the 5 and 25 wt.% CTAT polymerized samples ($w_{St}/w_{CTAT} = 0.1$). Small polystyrene rods are observed with aspect ratios much smaller than those of the parent wormlike micelles in the 5 wt.% sample (Fig. 8). Notice that the structures in the polymerized sample are wider and longer than the wormlike micelles of the original structure (inset in Fig. 8). By contrast, in the high surfactant-content sample, two types of structures are seen: polystyrene

cylinders of about 4 nm in diameter and 100 nm in length and spherical polystyrene particles of approximate 10 nm in diameters (Fig. 9). Also for comparison, a TEM photograph of the un-polymerized sample is included in the inset of Fig. 9. The formation of spherical micelles containing the solubilized styrene molecules in equilibrium with rod-like ones has been reported in literature [29, 30]. This may explain the reduction in G' and G'' when styrene was added to the surfactant solution.

Concluding remarks

The polymerization of styrene solubilized in CTAT wormlike micelles is reported. UV spectroscopy revealed that in the 0.05 wt.% CTAT system, styrene is located both at the micelle surface and in the hydrophobic core, whereas in the 0.5 wt.% CTAT system the monomer is mainly in the micelle core. SAXS and rheology suggests that the structure is preserved upon addition of styrene but the micelles become shorter upon solubilization of this monomer. The polymerization of styrene in these micelles follows a second-order kinetics, which implies that bimolecular reaction termination is the controlling termination mechanism. TEM and rheology disclose that upon polymerization, shorter rods (compared to the original parent wormlike micelles) are produced, which coexist with wormlike micelles form from the excess surfactant that is not adsorbed upon the polymer rods.

Acknowledgements This work was supported by the Consejo Nacional de Ciencia y Tecnología de México (Grants 38681-E and NC-204) and for the Spanish government through the Iberoamerica Scientific Cooperation Program. The authors thank the transmission electron microscopy technical support of Serveis Científico-Tècnics of the University of Barcelona and the technical assistance of Dr. Dámaso Navarro and Ms. Hortensia Maldonado of the Centro de Investigación en Química Aplicada (Saltillo, México) for the molar masses determinations.

References

1. Laughin RG (1994) The aqueous phase behavior of surfactants. Academic Press, London
2. Jönsson B, Lindman B, Holmberg K, Kronberg B (1998) Surfactants and polymers in aqueous solution. Wiley, New York
3. Israelachvili JN (1992) Intermolecular and surface forces. Academic Press, London
4. Paleos CM (ed.) (1992) Polymerization in organized media. Gordon Breach, Philadelphia
5. Thundathil R, Stoffer JO, Friberg SE (1980) J Polym Sci Polym Phys 18:2629
6. McGrath KM, Drummond CJ (1996) Colloid Poym Sci 274:316
7. McGrath KM (1996) Colloid Polym Sci 274:399
8. Guyot A (1996) Curr Opin Colloid Interface Sci 1(5):580
9. McKelvey CA, Kaler EW, Zasadzinski JA, Coldren B, Jung H-T (2000) Langmuir 16:8285
10. Gan LA, Lee KC, Chew CH, Ng SC (1995) Langmuir 11:449
11. Gan LA, Li TD, Chew CH, Teo WK (1995) Langmuir 11:3316
12. Rehage H, Hoffmann H (1982) Rheol Acta 21:561
13. Rehage H, Hoffmann H (1991) Mol Phys 74:933
14. Cates ME, Candau SJ (1990) J Phys: Condens Matter 2:6869
15. Soltero JFA, Puig JE, Manero O (1996) Langmuir 12:2654
16. Soltero JFA, Bautista F, Puig JE, Manero O (1999) Langmuir 15:1604
17. Lerebours B, Perly B, Pileni MP (1988) Chem Phys Lett 147:503
18. Kline S R (1999) Langmuir 15:2726
19. Soltero JFA, Puig JE Manero O, Schulz PC (1995) Langmuir 11:3337
20. Mukerjee P, Cardinal JR (1978) J Phys Chem 82:1620
21. Cardinal JR, Mukerjee P (1978) J Phys Chem 82:1614
22. Morini MA, Minardi RM, Schulz PC, Puig JE, Rodríguez JL (1998) Colloid Polym Sci 276:738
23. Schulz PC, Minardi RM, Vuano B (1998) Colloid Polym Sci 276:278
24. Mukerjee P (1975) In: Van Olphen H, Mysels KJ (eds) Physical chemistry: enriching topics from colloid and surface science. IUPAC, Theorex, La Jolla, California, p 135
25. Bohlm DS (1990) Diss Abs Int Ser B 51:1946
26. Zemb TN, Hyde ST, Derian PJ, Barnes IS, Ninham BW (1987) J Phys Chem 94:3814
27. Mukerjee P (1967) Adv Colloid Interface Sci 1:241
28. Odian G (1991) Principles of polymerization. Wiley, New York
29. Smith MB, Alexander AE (1957) Proc 2nd Int Congr Surface Activity, vol 1. Butterworths, London,p 311
30. EriksonJC, Gillberg G (1966) Acta Chem Scand 20:2019